1 *Article*

2 # Introduction of an experimental terrestrial
3 # forecasting/monitoring system at regional to
4 # continental scales based on the Terrestrial System
5 # Modeling Platform (v1.1.0)

6 **Stefan Kollet[1,2,*], Fabian Gasper[1,2,**], Slavko Brdar[3,2], Klaus Goergen[1,2], Harrie-Jan**
7 **Hendricks-Franssen[1,2], Jessica Keune[1,4,2,***], Wolfgang Kurtz[1,2,****], Volker Küll[4], Florian**
8 **Pappenberger[5], Stefan Poll[4], Silke Trömel[4], Prabhakar Shrestha[4], Clemens Simmer[4,2], and Mauro**
9 **Sulis[4,*****]**

10 [1] Agrosphere Inst., IBG-3, Inst. of Bio-Geosciences, Forschungszentrum Jülich GmbH, Jülich, Germany
11 [2] Centre for High-Performance Scientific Computing, Geoverbund ABC/J, Germany
12 [3] Jülich Supercomputing Centre, Forschungszentrum Jülich GmbH, Jülich, Germany
13 [4] Meteorological Institute, Bonn University, Germany
14 [5] European Centre for Medium-Range Weather Forecasts
15 * Correspondence: s.kollet@fz-juelich.de; Tel.: +49-2461-61-9593
16 ** Now at CISS TDI GmbH, Sinzig, Germany
17 *** Now at the Department of Forest and Water Management, Ghent University, Belgium
18 **** Now at Environmental Computing Group, Leibnitz Supercomputing Centre, Germany
19 ***** Now at the Department of Environmental Research and Innovation, Luxembourg Institute of
20   Technology, Luxembourg

21

22

23 **Abstract:** Operational weather and also flood forecasting has been performed successfully for
24 decades and is of great socioeconomic importance. Up to now, forecast products focus on
25 atmospheric variables, such as precipitation, air temperature and, in hydrology, on river discharge.
26 Considering the full terrestrial system from groundwater across the land surface into the
27 atmosphere, a number of important hydrologic variables are missing especially with regard to the
28 shallow and deeper subsurface (e.g. groundwater), which are gaining considerable attention in the
29 context of global change. In this study, we propose a terrestrial monitoring/forecasting system
30 using the Terrestrial Systems Modeling Platform (TSMP) that predicts all essential states and fluxes
31 of the terrestrial hydrologic and energy cycles from groundwater into the atmosphere. Closure of
32 the terrestrial cycles provides a physically consistent picture of the terrestrial system in TSMP.
33 TSMP has been implemented over a regional domain over North Rhine-Westphalia and a
34 continental domain over European in a real-time forecast/monitoring workflow. Applying a
35 real-time forecasting/monitoring workflow over both domains, experimental forecasts are being
36 produced with different lead times since the beginning of 2016. Real-time forecast/monitoring
37 products encompass all compartments of the terrestrial system including additional hydrologic
38 variables, such as plant available soil water, groundwater table depth, and groundwater recharge
39 and storage.

40 **Keywords:** terrestrial modeling; real-time forecasting/monitoring; workflows

41

42 ## 1. Introduction

43 Weather forecasting operates at global and local scale providing predictions into the future
44 from minutes, hours, and days to months on spatial scales from 100 meters to several kilometers [1].

45   Most national weather services such as e.g. the German national weather service DWD (Deutscher
46   Wetterdienst) [2] and the European Centre for Medium-Range Weather Forecasts [3] develop and
47   operate such forecasting systems. Weather forecasting systems constitute a major infrastructure
48   consisting of state-of-the-art software stacks and supercomputing hardware technologies, real-time
49   data streams of in-situ and remotely sensed observations, and global data exchange infrastructures
50   [4]. In operational forecasting, the software stack consists of a number of sophisticated components
51   including pre- and post-processing tools, the numerical weather prediction (NWP) model, and data
52   assimilation (DA) software, which constitute the kernel of the prediction system and comprise
53   decades of natural science findings and scientific software design knowledge (e.g. [3], [5-7]). In
54   essence, these prediction systems provide real-time forecasts of the states and fluxes in the
55   atmosphere based on a set of initial conditions and, in case of regional forecasts, lateral boundary
56   conditions, which are continuously corrected with observations applying data assimilation. In many
57   atmospheric centers, the software stacks are implemented on some of the most powerful parallel
58   computing and storage hardware available today providing the required capacity and redundancy.
59   Therefore, in terms of operational forecasting, the national weather services represent the
60   state-of-the-art [5]. In addition, there exists a large number of post-processed products of available
61   institutional numerical weather prediction simulation results, so-called re-analyses.

62   Similarly, in hydrologic forecasting of flood events, numerical hydrologic ensemble prediction
63   systems (HEPSs) are paired with DA technologies in operational forecasting frameworks similar to
64   NWP systems briefly outlined above [8-11]. A number of HEPS exist around the world (see for
65   example, EFAS, the European Flood Alert System center [9] and the NOAA National Water Model in
66   the US). In the hydrologic forecast realm, agricultural drought prediction receives attention and
67   poses a number of additional scientific and applied challenges, because of long-term memory effects
68   in the physical processes and scarcity of observations [12]. Often, drought information is made
69   available in so-called drought monitors, which provide recent hindsight information
70   (http://droughtmonitor.unl.edu/) based on input from NWP and atmospheric reanalysis products. It
71   is important that drought forecasts extend further into the vadose zone and groundwater because
72   these compartments constitute essential water storages relevant for e.g. public water supply,
73   agriculture and industry. While water resources management is considered a hot topic worldwide,
74   only very few operational, real-time water resources prediction system are implemented in an
75   institutionalized fashion online today. Examples include The Netherlands Hydrologic Instrument
76   [13] and the US National Water Model, which however does not include the groundwater
77   compartment and focuses on stream discharge and land surface variables (http://water.noaa.gov/).

78   In summary, juxtaposing NWP and HEPS, we note that while there is a plethora of literature on
79   even real-time HEPSs in the scientific community, the large majority of HEPS developments and
80   applications remain in the scientific realm and have not been operationalized. Moreover, NWP and
81   HEPS compartmentalize the earth system into the atmosphere and land surface-soil domains instead
82   of providing a complete and physically consistent forecast of the water, energy and momentum
83   cycles from the bedrock to the top of the atmosphere. In addition, the groundwater compartment is
84   generally missing in the simulations. The situation is, of course, rooted in the complexity and
85   sometimes limited understanding of the system, the lack of adequate computing resources, the
86   objectives of the specific forecast, and legislative mandates.

87   As a result, consistent forecasts of the complete terrestrial water and energy cycle from
88   groundwater across the land surface into the atmosphere at scientific and socioeconomic relevant
89   space and time scales are missing. This also holds for the current state of water resources, which is
90   generally only known from sparse, local in-situ observations and temporal snapshots from remote
91   sensing of the land surface. Thus, society is exposed to a large degree of uncertainty with respect to
92   the current and future state of freshwater resources, the future trajectory of water use and
93   management, and water related hazards, such as floods and droughts.

94   In this paper, we present an implementation of a fully automatized, regional to continental scale
95   forecasting/monitoring system from groundwater into the atmosphere based on the Terrestrial
96   Systems Modeling Platform, TSMP [14, 15]. The overarching goal of the system is to extend the

97 atmospheric-centric view of forecasting to the complete terrestrial ecohydrological system
98 ultimately including the biosphere. TSMP, developed within the framework of the Transregional
99 Collaborative Research Centre TR32 [16] has been applied in a wide variety of studies ranging from
100 the regional to the continental scale with generally reasonable agreement to observations [17-21]. In
101 addition, human water use has been implemented also assessing the potential added value in the
102 comparison to precipitation and evapotranspiration products [22, 23].
103   In this study, the term monitoring system is preferred, in order to emphasize the reciprocity of
104 model based simulations and observations in the application of data assimilation technologies:
105 Models are used to interpolate (in space and time) between observations to provide information
106 everywhere and at any time, while observations are used to correct the simulations acknowledging
107 model and observational uncertainties. Currently, the monitoring system produces time lapse
108 images of all relevant states and fluxes of the terrestrial water and energy cycle (table 1) at the
109 applied model resolution including uncertainty estimates. The system is considered as a blueprint of
110 an operational system ultimately merging all available observations from the subsurface to the
111 atmosphere with a physics-based, high-resolution terrestrial model providing best estimates of the
112 current state of the system and used to generate forecasts/projections at resolutions relevant for
113 scientists and stakeholders. Here, we highlight technical requirements, the experimental design, and
114 considerations on improving prediction accuracy with precipitation radar integration as preliminary
115 steps to data assimilation. In the following, we outline and describe the components of the
116 monitoring system, provide information on the workflow and details of the automatization,
117 example forecast products, and a discussion of the path forward.
118
119   Table 1. Selected essential states and fluxes simulated by the terrestrial monitoring system.
120

Variable name	Units
Subsurface hydraulic pressure	[m]
Subsurface relative saturation	[-]
Subsurface Darcy flow	[mh^{-1}]
Overland flow, surface runoff	[ms^{-1}]
Evaportranspiration	[mms^{-1}] or [Wm^{-2}]
Sensible heat	[Wm^{-2}]
Ground heat	[Wm^{-2}]
Long/short wave radiation (incoming and outgoing)	[Wm^{-2}]
Precipitation (liquid and frozen)	[mms^{-1}]
Snow water equivalent	[m]
Barometric pressure	[Pa]
Air temperature	[K]
Air humidity	[kgkg^{-1}]
Air wind speeds	[ms^{-1}]
Cloud cover	[-]

121

2. Materials and Methods: Terrestrial Monitoring System's components and domains

123 The kernel of the Terrestrial Monitoring System (TMS) consists of a number of simulation software
124 and hardware components, and data streams, which are linked in a scripted, automated workflow
125 (Section 3). The software components encompass the actual forward or forecast model TSMP
126 (Terrestrial Systems Modeling Platform), which has been proposed by [14] and installed at a Linux

127   cluster of the Jülich Supercomputing Centre. TSMP has been implemented over a regional and
128   continental model domain, which are slightly smaller than North-Rhine Westphalia (NRW) and
129   larger than the pan-European domain (EU), respectively (Figure 1). Additionally, the hydrologic
130   state of the NRW model is corrected with the help of precipitation-radar observations to improve
131   model initialization and the ensuing forecast products. The TMS follows a specific monitoring clock,
132   which is mainly determined by the availability of boundary conditions from operational weather
133   forecasting centers and observation periods. Finally, a number of monitoring products are produced
134   and published online.

135
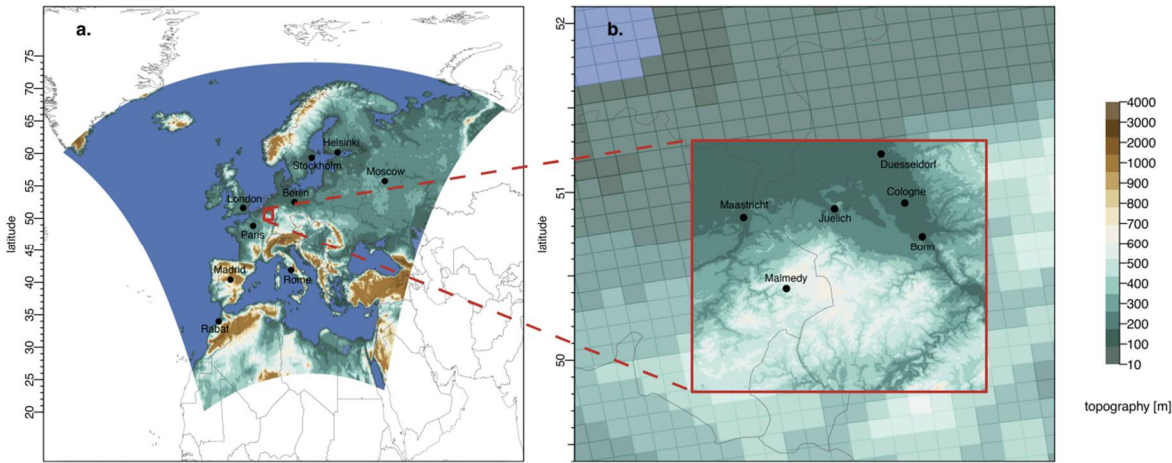
136
137   **Figure 1.** The monitoring domains European (EU, left) and North-Rhine Westphalia (NRW, right).
138   Black circles indicate capitals and major cities of the simulation domains. The domain highlighted in
139   red in the figure on the right is the Rur catchment, which is highly equipped with hydrological and
140   hydrometeorological measurement equipment.

141

142   *2.1 Software and hardware components of the Terrestrial Monitoring System, TMS*

143   The dynamic kernel of the TMS is the parallel Terrestrial Systems Modeling Platform
144   (TerrSysMPv1.1.0), which is a scale-consistent, fully integrated groundwater-to-atmosphere model,
145   conserving moisture and energy across all compartments of the geo-ecosystem for different
146   domains. TSMP consists of the numerical weather prediction system (COSMO, v4.21) of the German
147   national weather service (DWD, [24]), the Community Land Model (CLM, v3.5) [25], and the
148   variably saturated surface–subsurface flow code ParFlow (v3.1) [26-28]. The interested reader is
149   referred to the aforementioned publications and [14] for a detailed description of the modeling
150   system. In order to exchange fluxes and states across the individual component models of TSMP and
151   close the terrestrial water and energy cycle, the Ocean-Atmosphere-Sea-Ice-Soil coupler,
152   OASIS3-MCT [29] is used. In a massively parallel supercomputing environment, the portation,
153   profiling, optimization and scalability of TSMP has been documented in [15]. The unique feature of
154   TSMP is that all states and fluxes of the terrestrial water and energy cycle from groundwater across
155   the land surface into the atmosphere are simulated in a mass and energy conservative and scale
156   consistent implementation. Thus, the platform provides simultaneously consistent predictions in all
157   terrestrial compartments, i.e. the subsurface, land surface, and atmosphere.
158   In the current setup, which is running continuously since January 2016, the bulk of the
159   monitoring simulations are performed on JURECA, the Jülich Research on Exascale Cluster
160   Architecture. JURECA is a 1872 node (45,216 cores) supercomputer based on T-Platforms V-class

161 server architecture with a peak performance of 1.8 (CPU) + 0.44 (GPU) Petaflops per second. The
162 nodes consist of two 12 core Intel Xeon E5-2680 v3 Haswell CPUs and three different DDR4 memory
163 configurations (128GB, 256GB, 512GB), which are connected through a Mellanox EDR Infiniband
164 network with fat tree topology and a 100GB per second connection to the GPFS storage cluster.
165   The cluster uses the CentOS 7 Linux distribution as operating system and handles the resource
166 management with the Slurm batch system and Parastation. Also relevant for this work is the fact that
167 cronjobs (tasks scheduled in the background) are prohibited, ssh (secure shell) connections are
168 secured by RSA key-pairs, and compute nodes do not have internet access. This is commonly the
169 case in supercomputing environments, which are not designed and operated for operational use,
170 and must be taken into account in the design of the workflow. The maximum wallclock time is 24
171 hours and maintenance downtime affects the whole system for several hours on a regular basis (on
172 demand 1-2 per month).
173   Part of the ensemble simulations of the NRW domain were performed on JUQUEEN, JSCs 5.0
174 Petaflop IBM Blue Gene/Q supercomputer with 458752 cores and 448TB main memory. JUQUEENs
175 28 racks are further divided into 32 nodeboards, which are the smallest allocatable units, each
176 consisting of 32 nodes with 16 IBM PowerPC A2 CPU cores (4-way simultaneous multithreading).
177 Each node has 16 GB DDR3 SDRAM and is connected through a 5-D torus (4x4x4x4x2 configuration)
178 network with very high peak bandwidth (40GB s-1). JUQUEENs job submissions are handled by the
179 LoadLeveler job scheduling system. JUQUEEN has been decommissioned in May 2019 and replaced
180 by a new supercomputing architecture, which will be used to generate the ensemble in future.
181

182 *2.2 Software and hardware components of the Terrestrial Monitoring System, TMS*

183 *The North-Rhine Westphalia domain*
184   The regional scale domain (Figure 1) covers the south-western part of Germany's North
185 Rhine-Westphalia (NRW) including parts of Belgium, Luxembourg, and the Netherlands. NRW
186 contains the catchments of the rivers Rur, Erft and Swist and partially Rhine, Moselle and Meuse.
187 The domain is 150x150km large and has a convection permitting resolution of 1km for the
188 atmosphere and 0.5km for the land surface and subsurface resulting in a 150x150 and 300x300 grid
189 size, respectively, with regard to nx and ny, respectively. The number of cells in vertical dimension
190 is nz=30 for ParFlow, nz=10 for CLM, and nz=50 for COSMO. In the atmospheric model COSMO, the
191 time step size is determined by the spatial discretization and set to dt=10s. Time integration of the
192 relevant exchange fluxes with the land surface and subsurface model CLM and ParFlow is
193 performed by OASIS3-MCT in a 900s interval, which is also the time step size of CLM and ParFlow
194 and the coupling time step between COSMO, CLM and ParFlow. Between 2016 and 2018, the
195 atmospheric initial condition and hourly boundary conditions were provided daily by a
196 deterministic forecasting run of the DWD, uploaded to a FTP server at the Meteorological Institute
197 of the University of Bonn, and then ingested automatically to the TMS every 3h with a maximum
198 lead time of 25h. Note, in May 2018, DWD changed their data policy and provision, which resulted
199 in a hiatus in the boundary condition from the operational forecast. Currently, the NRW monitoring
200 system is adopted to ingest initial and boundary information from the 12.5km resolution European
201 monitoring system of ECMWF described below via a one-way nesting every 6 hours and with
202 maximum lead time of 72h. The hydrologic boundary and initial conditions are of the Dirichlet type
203 and obtained from the previous day's forecast, resulting in a continuous hydrologic time series.
204 Details of the parameterizations and physical parameter values can be found in [14] and [21].The
205 forecast is distributed over 2 nodes on JURECA and requires approximately 1h compute (wall-clock)
206 time. In a more recent development, the initial conditions are improved continuously via hindsight
207 simulations based on assimilated rain radar information, which is explained in Section 2.4.
208   In the groundwater-to-atmosphere simulations of the monitoring system, precipitation rates
209 and patterns are always a challenge to model [30]. In weather forecasting, incorrect precipitation
210 fields propagate into the water and energy fluxes of the lower land surface boundary condition that
211 are evapotranspiration and sensible heat, which in turn influence the aforementioned atmospheric

212 processes through two-way feedbacks. However, in the operational setup of the weather services,
213 this error propagation is alleviated via data assimilation, which constantly corrects the atmosphere
214 and land surface states by means of observational data during the assimilation phase of the forecast.
215 In contrast, in the current TMS incorrect precipitation fields are propagated directly into the land
216 surface and groundwater compartments, because of the fully coupled nature of the TMS and the lack
217 of strongly coupled data assimilation capabilities across the different terrestrial compartments,
218 which is still subject of scientific research [31, 32]. In a first correction step for the NRW domain, the
219 precipitation fields from the monitoring run are replaced by rain radar information from
220 high-resolution X-band radar composites at the end of the monitored day. While rain rates from
221 radar observations are also error prone, we expect an overall improvement in comparison to the
222 predicted rain rates from NWP. The observed rain rates in the atmospheric forcing data set are then
223 used to perform an offline subsurface-land surface hydrologic simulation in order to improve the
224 states and fluxes, and, thus, the initial condition for the following day with the observed rain rates.
225 This simulation is called correction run in the following sections.
226   The rain radar products covering the North-Rhine Westphalia (NRW) domain are provided by
227 the Meteorological Institute, Bonn University. They are composed of the measurements of the
228 polarimetric X-band radar at the Meteorological Institute in Bonn (BoXPol) and the polarimetric
229 X-band radar in Jülich (JuXPol), for technical details of the radar see [33]. The twin-radars provide
230 volume scans consisting of plan position indicators (PPIs) measured at different elevation angles
231 every 5min in order to monitor the 3D structure of precipitating clouds in the North-Rhine
232 Westphalia domain. The rain product is based on the lowest level of the 3D composite and is
233 transferred for ingestion into the monitoring system at the end of each day. For details of the rain
234 product the reader is referred to [34].
235
236 *The pan-European domain*
237   The continental scale pan-European domain (EU, Figure 1) conforms to the CORDEX EUR-11
238 standard, which is part of the World Climate Research Program, and covers Europe and parts of
239 northern Africa, western Russia and Asia. The domain is 5450x5300km large and discretized at a
240 resolution of 12.5km resulting in a 436x424 grid size with regard to nx and ny. The number of cells in
241 the vertical direction is nz=15 for ParFlow, nz=10 for CLM, and nz=50 for COSMO. The time step size
242 is set to dt = 60s for COSMO and dt = 1h for ParFlow and CLM which is also the coupling frequency.
243 The atmospheric initial conditions and hourly boundary conditions are provided on a daily basis
244 from a high-resolution forecasting run of the European Centre for Medium-Range Weather
245 Forecasts (ECMWF). The hydrologic initial conditions and boundary conditions are obtained from
246 the previous day's forecast resulting in a continuous hydrologic time series. Due to potential biases
247 drifts in hydrologic states and fluxes may occur that have not been diagnosed so far. Details of the
248 parameterizations and physical input parameter values can be found in Keune et al. (2016). A
249 forecast of 72h is performed that is distributed over 6 JURECA nodes and requires approximately
250 1.5h compute (wall-clock) time.
251

252 *2.3 Monitoring Clock*

253   Figure 2 shows the monitoring clock i.e. the timeline of the workflows for the NRW and EU
254 domain (Section 3) that is executed automatically on a daily basis. Both workflows are the same
255 except for the precipitation radar correction, which is only applied for NRW, and the provision of
256 the atmospheric initial and boundary condition information, which is provided from the DWD and
257 ECMWF for NRW and EU, respectively. In case of NRW, the monitoring clock starts with the
258 retrieval of the precipitation radar products of the University of Bonn shortly after midnight UTC
259 followed by the correction run of the previous day. This run usually requires less than 1h compute
260 time. DWD's and ECMWF's initial and boundary conditions are made available around 02:00 UTC
261 and preprocessing starts after the retrieval of the files from a ftp-server. The actual monitoring runs
262 with TSMP commence as soon as the initial and boundary conditions are preprocessed (around

263   02:15 UTC). The TSMP runs usually require between 1 and 1:30h. In an ensuing step, post-processing
264   is performed and forecasts are made publicly available via videos on YouTube around 03:45 UTC
265   (see Section 3.1). The start of scripts is automatically postponed if required preceding steps are not
266   completed or in case of missing initial and boundary information. The different steps of the
267   monitoring clock are detailed in section 3.
268
269
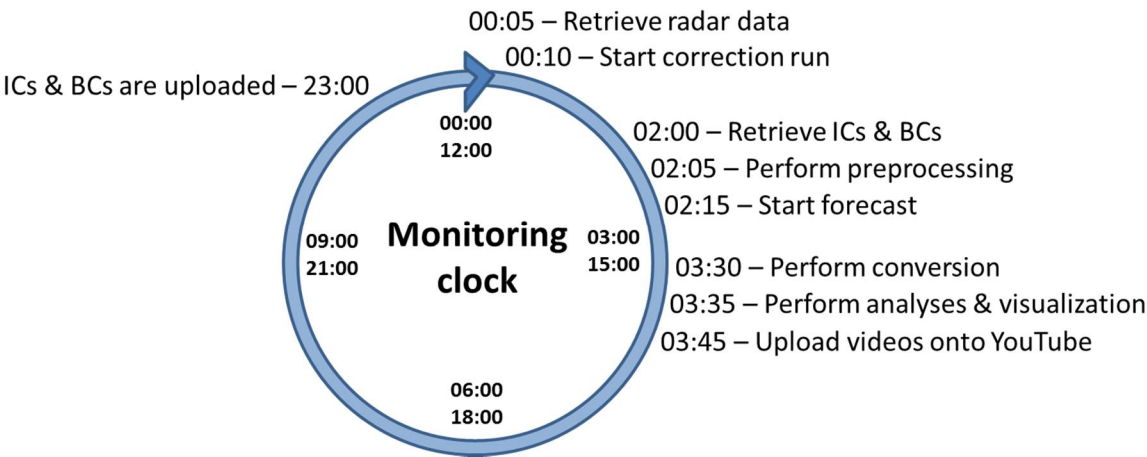
272   **Figure 2.** Schematic of the monitoring clock for the NRW and EU domain. Note, the rain radar
273   correction is only performed in case of the NRW domain (ICs: Initial conditions; BCs: Boundary
274   conditions).
275

3. Workflows and automatization

277   In this section, the workflow for creating a model run and its technical implementation is
278   described including pre- and post-processing. In addition, the precipitation radar correction
279   approach is outlined in more detail.

3.1 Monitoring EU and NRW

281   The monitoring workflow for the EU and NRW domains consists of sequentially executed steps
282   detailed below and in Figure 3. Note, both monitoring runs, NRW and EU are based on the same
283   workflow implemented on the supercomputer JURECA of the Jülich Supercomputing Centre. The
284   flowchart in Figure 3 is valid for EU and NRW with some added complexity due to the precipitation
285   radar correction in case of NRW as aforementioned (see Section 3.2 and Figure 4).
286
287

288
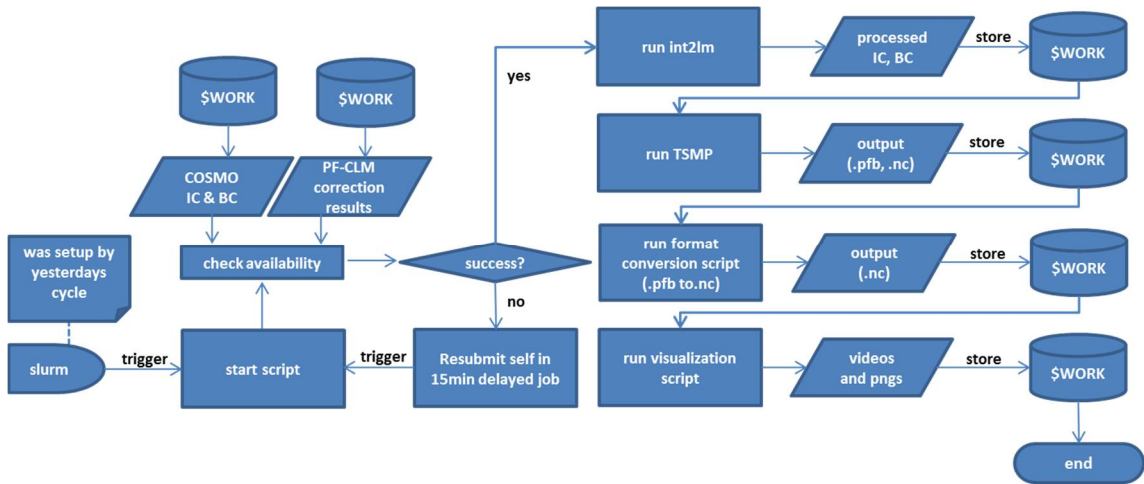
289 **Figure 3.** Flowchart for both the EU and NRW monitoring system implemented in the forecast
290 jobscript running on the compute nodes of JURECA, Jülich Supercomputing Centre (JSC). Note that
291 both monitoring runs are based on the same workflow.
292
293 *Retrieval of boundary and initial conditions* - All partial differential equation based models require
294 initial and boundary conditions to close the mathematical problem. In TSMP, the hydrologic model
295 ParFlow has fixed boundary conditions of the Neumann and Dirichlet type in case of the EU and
296 NRW domains, and a free overland flow boundary condition at the land surface. Initial conditions
297 are obtained from the previous day's run and from the correction run applying the precipitation
298 radar information in case of NRW. The lateral boundary condition for COSMO is read from a forcing
299 file which was obtained by the nesting approach starting from a global NWP model. These
300 boundary conditions together with the initial condition are provided by DWD (for the NRW
301 domain) and ECMWF (for the CORDEX EUR-11 domain) and downloaded from the corresponding
302 FTP-servers.
303
304 *Preprocessing* - The initial and boundary conditions are obtained from the corresponding global
305 weather prediction systems with a grid spacing of 2.8km and approximately 12km from DWD and
306 ECMWF, respectively. These products are then interpolated to the desired resolution - 1km for NRW
307 and 12.5km für CORDEX EUR-11 - and cropped to the final domain size. Boundary conditions for
308 both domains are created by interpolation. This is done by the standard preprocessing tool int2lm (v.
309 2.01, [35]) for the COSMO model. The tool interpolates the initial and boundary condition (in Grib or
310 NetCDF format) from a coarser source grid and/or larger domain into the desired destination grid.
311 In addition, int2lm renames and transforms all arrays and parameters into a COSMO-readable
312 format, therefore both, DWD data as well as ECMWF data, needs to get preprocessed by int2lm.
313
314 *Forward simulation* - The monitoring system with TSMP is designed to perform continuous, real-time
315 monitoring simulations. Nevertheless, the NWP model COSMO is driven by the aforementioned
316 downloaded and preprocessed initial and boundary conditions and, thus, reinitialized every day.
317 The surface/subsurface models CLM and ParFlow, on the other hand, are restarted with the restart
318 files, which were generated by the previous day's simulation cycle. Due to the slow dynamics in the
319 surface/subsurface, the hydrologic model (i.e. ParFlow-CLM) needs an extended spinup simulation
320 with real meteorological forcing before the states are in a physically consistent dynamic equilibrium.
321 This spinup was also performed for both domains in advance to the real-time monitoring. By
322 running the monitoring system continuously, the equilibrium between the subsurface, land surface
323 and atmosphere is maintained and automatically extended. All component models of TSMP have
324 their own set of parameter files, usually called namelists (traditional Fortran nomenclature), that
325 define a large set of runtime information and parameterizations. Several input information that is
326 necessary for daily forecast runs, like dates, path to forcing files, run directories or output folders
327 must be consistently set up across all namelists. This is possible in a formalized and consistent
328 manner for the three model components by implementing a setup script environment.
329
330 *Postprocessing and visualization* - The component models of TSMP generate output files in different
331 formats (ParFlow binary, PFB, and NetCDF) in hourly intervals. An NCL script (NCAR command
332 language) converts PFB to NetCDF and aggregates hourly input into one single file for additional
333 post-processing and ensuing archiving. The analyses and visualization are done by a set of Python
334 scripts, which read the output files generated by TSMP with the NetCDF4 Python library in a first
335 step. The output from, for example, ParFlow only consists of pressure and saturation for a given
336 domain. Together with static fields, the data is then post-processed to the desired analyses, such as
337 surface runoff, groundwater recharge, plant available water, and groundwater table depth. Also
338 standard meteorological products and analyses, such as wind speed, temperature, precipitation, and
339 geopotential heights of pressure levels are generated. After the analysis of output variables is
340 completed, frames for each individual analysis and time step (hourly) are plotted to PNG files with

341   the Python libraries matplotlib and basemap. These PNG files are then rendered with ffmpeg into an
342   AVI-movie.
343
344   *YouTube upload and archiving* - After all previous steps are finished, the generated movies are
345   uploaded via Google API v3 into the corresponding YouTube playlist. Data for the web-app is
346   copied to a webserver and the whole experiment folder is zipped and moved into archive. The raw
347   data is available for at least 10 years.
348
349   Note that the five steps outlined above are contained in three scripts which are triggered by
350   cronjobs on a different machine over ssh, because user cronjobs are not allowed on JURECA. The
351   data retrieval step and upload/backup step are triggered by separate scripts/cronjobs on the
352   JURECA front nodes and are separated from other steps because the JURECA compute nodes are
353   not connected to the internet. The simulations are set up by a third script/cronjob, which also
354   submits the jobscript to JURECAs job scheduler (slurm) for handling preprocessing, model run and
355   visualization. These scripts contain several reliability mechanisms. For example, delayed scripts
356   restart if download files or checkpoint files are not present, accommodating maintenance
357   downtimes, automatically catching stalled runs and handling jobscripts with 24h lead time in order
358   to optimize job queue position. The overall availability and reliability of the system completely
359   depends on the availability and reliability of the supercomputing resources of JSC. Regular and
360   unplanned system maintenances directly impact the monitoring system and resulting forecast. At
361   this point, no redundancy has been implemented.

362   *3.1 Precipitation radar integration for NRW*

363   As mentioned above and in Section 2, the surface and subsurface models CLM and ParFlow are
364   restarted utilizing the results/restart files of the previous day. This introduces errors due to
365   inaccuracies in the prediction of water fluxes in the groundwater-to-atmosphere system, especially
366   with regard to precipitation. In order to improve the hydrologic states, precipitation radar
367   information is applied in a correction run in an extension of the workflow for NRW (Figure 4).
368
369   *Radar data retrieval and preprocessing* - The radar data is accessible on a server of the Meteorological
370   Institute, Bonn University, and is downloaded shortly after midnight. The radar data are available as
371   NetCDF files and are generated every 5 minutes. The grid of the radar data has the same resolution
372   as the forecast run (1km) therefore no interpolation is needed. Because the radar data covers a much
373   larger domain, the data needs to be cropped to the NRW grid sizes. Offline forcing files (i.e. time
374   series of radiation, air temperature, precipitation, wind speeds, barometric pressure and specific
375   humidity at each individual pixel) are newly generated from the model run, in which the radar rain
376   rates replace the simulated precipitation fields from the monitoring run.
377
378   *TSMP correction run and upload/archiving* - TSMP is run in CLM-ParFlow offline mode without
379   COSMO where the newly created forcing files are used as offline atmospheric forcing in CLM. The
380   remainder of the configuration is the same as in the forecasting run. The results are also zipped and
381   moved into the archive.
382
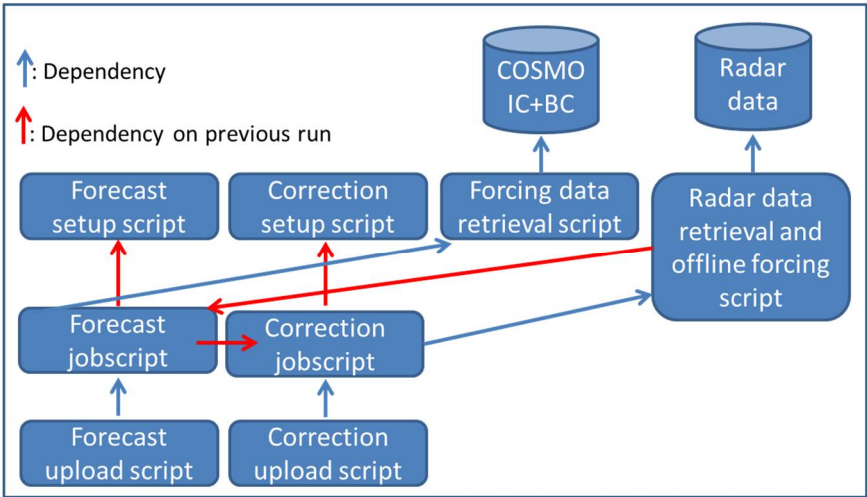
383
384   **Figure 4.** Schematic of the different dependencies between the tasks implemented in individual
385   workflow scripts of the correction run. Blue arrows indicate dependencies on the previous step in
386   the workflow, while red arrows indicate dependencies in the workflow on information from the
387   monitoring run of the previous day.

388   *3.3 Publication of monitoring products*

389   The results are disseminated on the video platform YouTube
390   (https://www.youtube.com/channel/UCGio3ckQwasR5a_kJo1GdOw). Instead of a locally
391   maintained web presence, YouTube is already established and has a strong impact especially
392   beyond the scientific community. It is free and easy to use and has synergies with other social media
393   making it easy to share, link or embed. Additionally, YouTube is fully controllable via a Python API,
394   which is important for the integration into the workflow and automatization process presented
395   above. YouTube provides limited but sufficient structuring features for our purposes, which were
396   used to arrange the daily results. The two domains are separated by playlist-sections where every
397   analysis is represented as playlist and new videos are added automatically. Additionally, we
398   developed a web-app particularly designed for mobile devices that allows displaying meteograms
399   of all analysis products for the current (or a manually selected) location
400   (www.terrsysmp.org/tsmp_app). The raw data is also available via sftp for the past three months.
401   Note, all data are published in an ad hoc fashion i.e. at this point no quality control has been
402   implemented.

403   **4. Results and discussion**

404   Running a fully integrated, groundwater-to-atmosphere terrestrial systems model in forecast
405   mode, opens up new opportunities. In addition to weather variables, special emphasis on the
406   analyses of hydrologic variables enables new applications that are unique so far. For example,
407   forecasted analyses of plant available water is useful for agricultural applications, surface runoff for
408   flood forecasting and hydropower, and groundwater recharge, water table depth and water column
409   storage for water resources management and drought prediction. In the following sections, example
410   results of the different monitoring experiments are shown.
411

412   *4.1 Monitoring EURO CORDEX and NRW*

413   In comparison to widely available meteorological forecasts, the unique feature of the
414   monitoring system are experimental analyses and monitoring products of all state variables and
415   fluxes from groundwater across the land surface into the atmosphere. A large number of variables
416   can be accessed at https://www.youtube.com/channel/UCGio3ckQwasR5a_kJo1GdOw. Below, some
417   examples are shown for more classical atmospheric products (Figure 5 and 6), a hydrologic variable
418   (Figure 7) over Europe during the heat wave of 2018, and hydrologic variables over NRW (Figure 8

419   and 9) during the flooding in January 2018, which are not commonly available. For example, Figure
420   9 shows groundwater recharge, which is a variable of great interest to public water managers and
421   agriculture.
422   Figure 5 shows the 2m air temperature over Europe on August 7th, which was the peak of the
423   heat wave in Germany in 2018. Temperatures above 35 °C were recorded in Germany during that
424   time period. In addition, meteograms are provided for the location of the city of Jülich, Germany, for
425   2m air temperature, sea level barometric pressure, 2m specific humidity, 20m wind speed, and
426   precipitation. Figure 6 shows the precipitation forecast over Europe including precipitation
427   meteograms for a number of European capitals. Both figures constitute standard NWP products.
428   Figure 7 shows the change in plant available soil water as a new product, which is the change in the
429   amount of water that is available to plants via root water uptake at a matric potential > 10m. The
430   figure illustrates the overall recession of plant available water on the order of -10mm over a period of
431   72h with localized recharge due to local precipitation events toward the end of the forecast period.
432
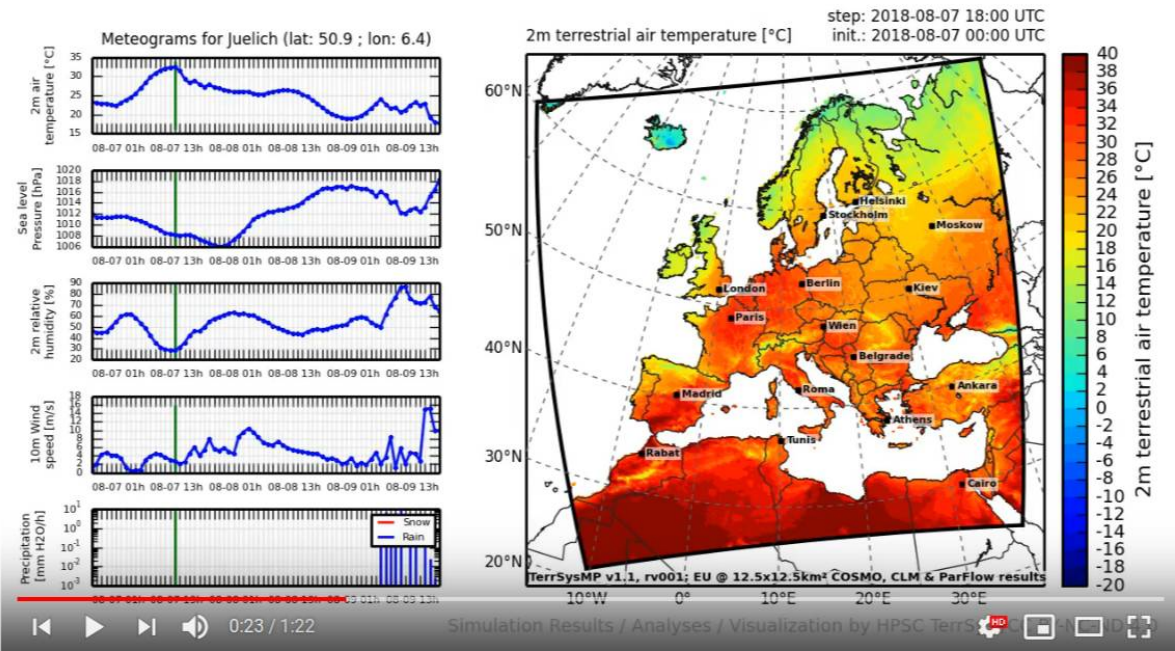
433
434
435   **Figure 5.** Monitoring output of TerrSysMP (CORDEX EUR-11 domain) for the terrestrial 2m air
436   temperature [°C] at the peak of the heat wave on August 7th, 2018. On the left from top to bottom,
437   the meteograms depict 2m air temperature [°C], sea level pressure [hPa], 10m wind speed [ms 1],
438   and precipitation [mmh-1] in Jülich (latitute:50.9, longitude: 6.4), Germany.
439
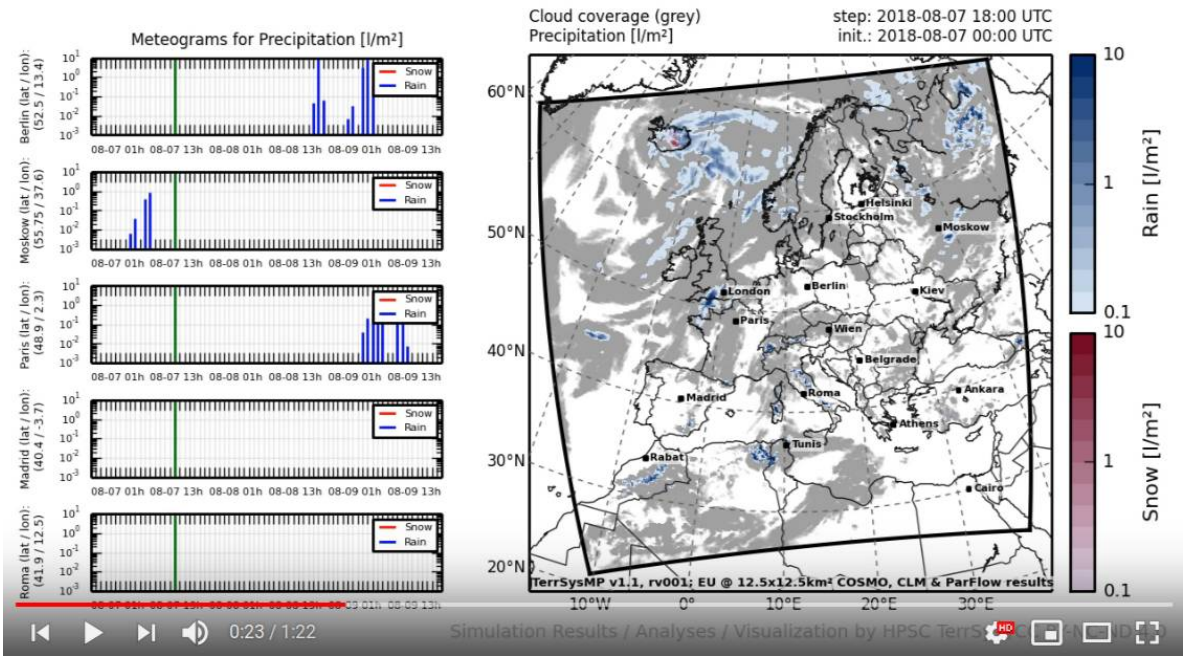
Figure 6. Monitoring output of TerrSysMP (CORDEX EUR-11 domain) for precipitation [lm-² or mm] in logarithmic scale on August 7th, 2018. On the left from top to bottom, the meteograms depict precipitation rates (snow and rain) [lm-² or mm] for the European capitals Berlin, Moscow, Paris, Madrid and Rome.
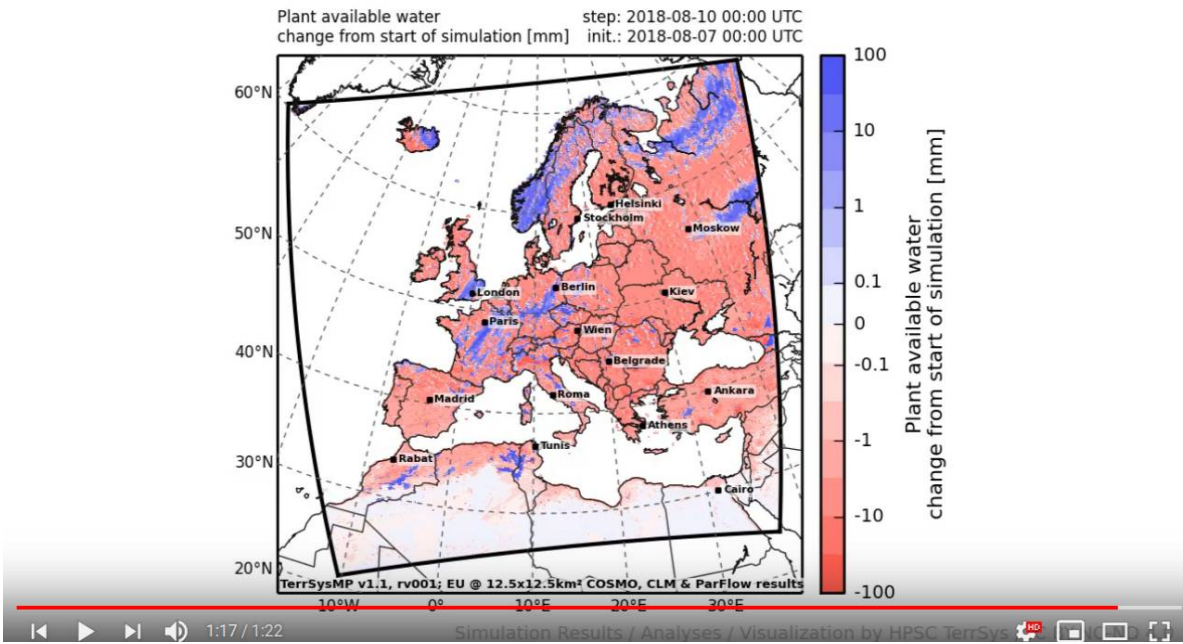
Figure 7. Monitoring output of TerrSysMP (CORDEX EUR-11 domain) of the change of plant available water [mm] over the course of the prediction period of 72h (between August 7 and August 10, 2018).

Figure 8 shows the change in groundwater table depth over the prediction period of 24h (8th of January, 2018) over the NRW domain. The forecast suggests widespread recession of groundwater (positive values) with increasing groundwater table depth and localized decreases in water table depth in recharge areas. This is in contrast to the flooding of the Rhine River during the same period, which was mainly caused by heavy precipitation and snow melt in Southern Germany and the Alps.

458   The predicted groundwater recharge shown in Figure 9 is spatially quite heterogeneous
459   contradicting the common assumption of spatially uniform recharge areas along topographic ridges
460   and heights. Especially in the Eifel region in the south of the monitoring domain, recharge areas
461   alternate with discharge areas over small distances, which is difficult to simulate with simplified
462   modeling approaches separating the groundwater compartment from the soil zone and land surface.
463
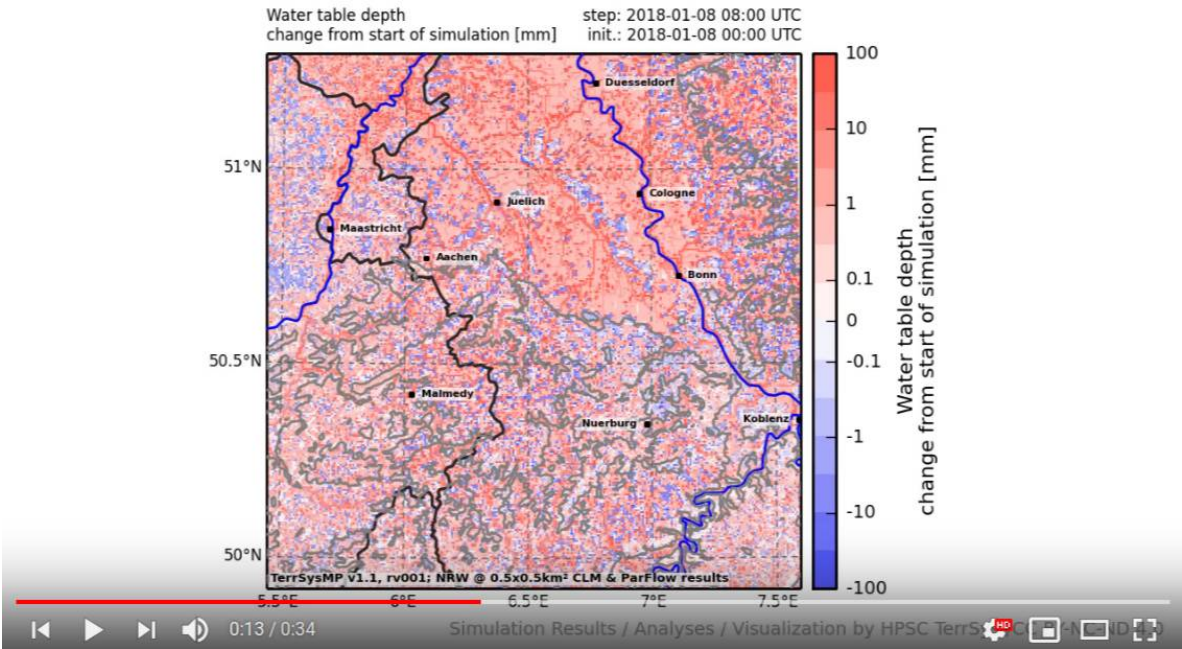
464
465
466   **Figure 8.** Monitoring output of TerrSysMP (NRW) for the water table depth change [mm] in
467   logarithmic scale. The change is estimated relative to the initialization at the beginning of the
468   monitoring run. Negative values indicate a rise of the water table.
469
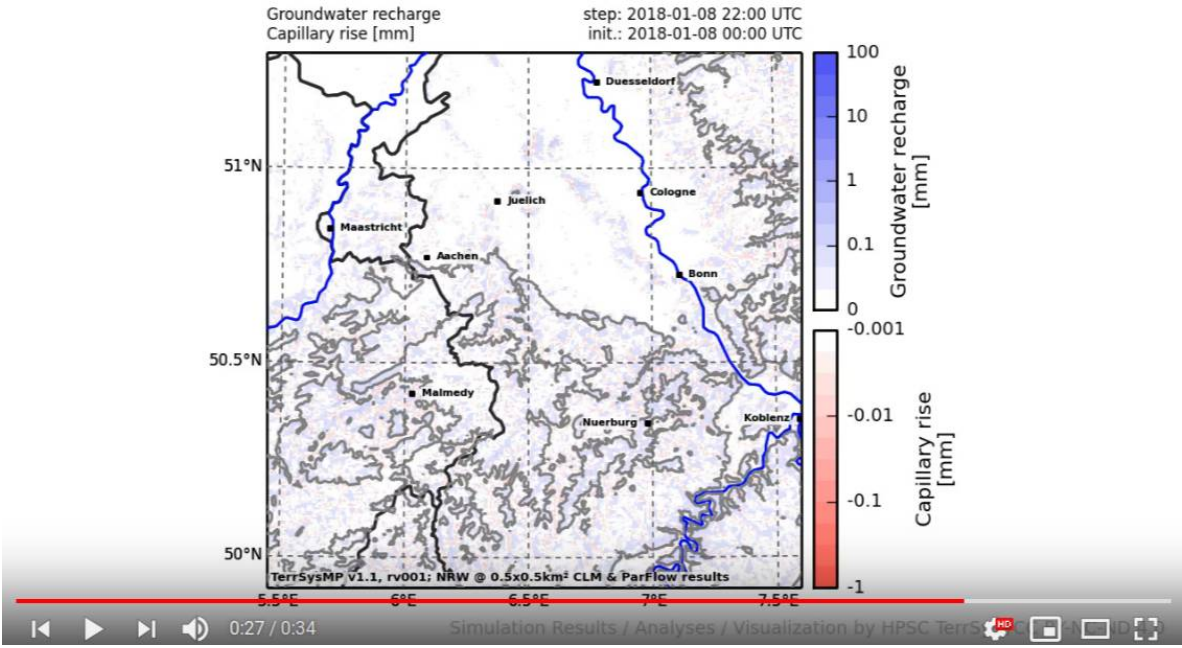
470
471
472   **Figure 9.** Monitoring output of TerrSysMP (NRW) for groundwater recharge (positive) and
473   capillary rise (negative) [mm] i.e. the plant available water storage change [mm (sym log)]. The
474   change is relative to the initialization step. The plant available water is the water that is stored in the
475   pore space at a matric potential large than -10m.
476

4.2 Radar correction for NRW

Figures 10 to 12 show the impact of the rain radar correction on the hydrology using the precipitation radar information as forcing in January 2018. Figure 10 shows the cumulative precipitation fields from the monitoring and correction run (small panels on the right), and the difference between both runs. One can clearly distinguish regions of over- and underestimation of precipitation, which results in correlated differences in air temperature (Figure 11) and, more pronounced, in surface runoff (Figure 12). While precipitation products from radars are error prone, we expect an improvement in the simulated states especially with regard to their spatial distribution.
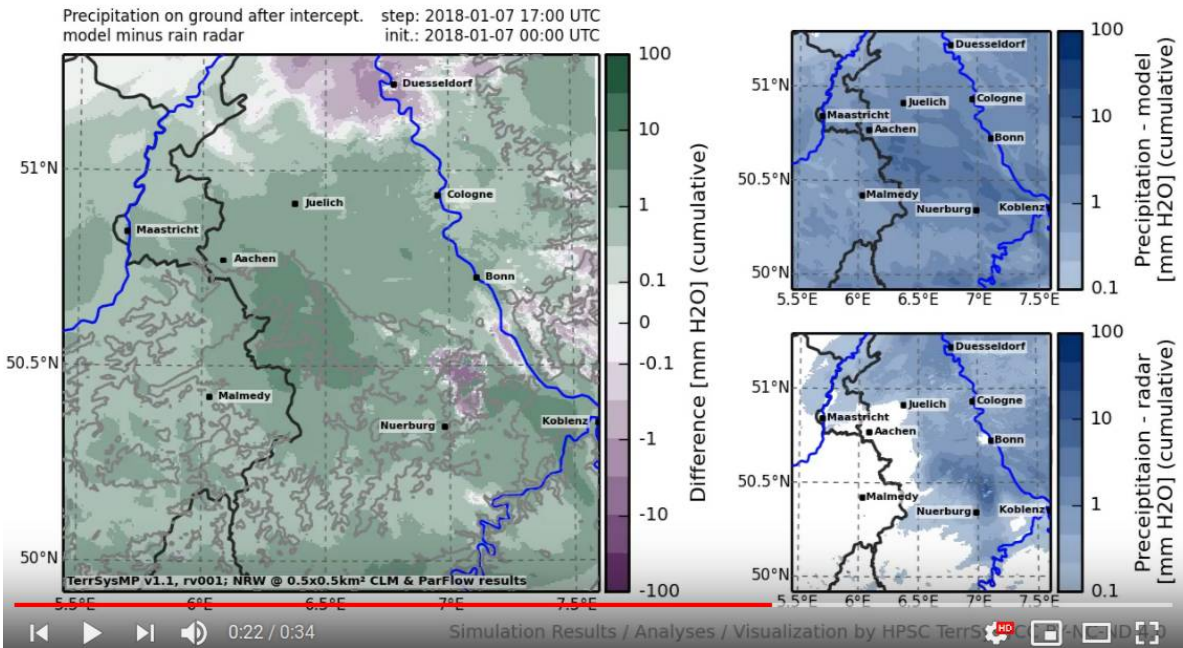
Figure 10. Difference plot for precipitation [mm] between simulated and radar precipitation (left). The panels on the right show the simulated precipitation (top) and radar-estimated precipitation (bottom).
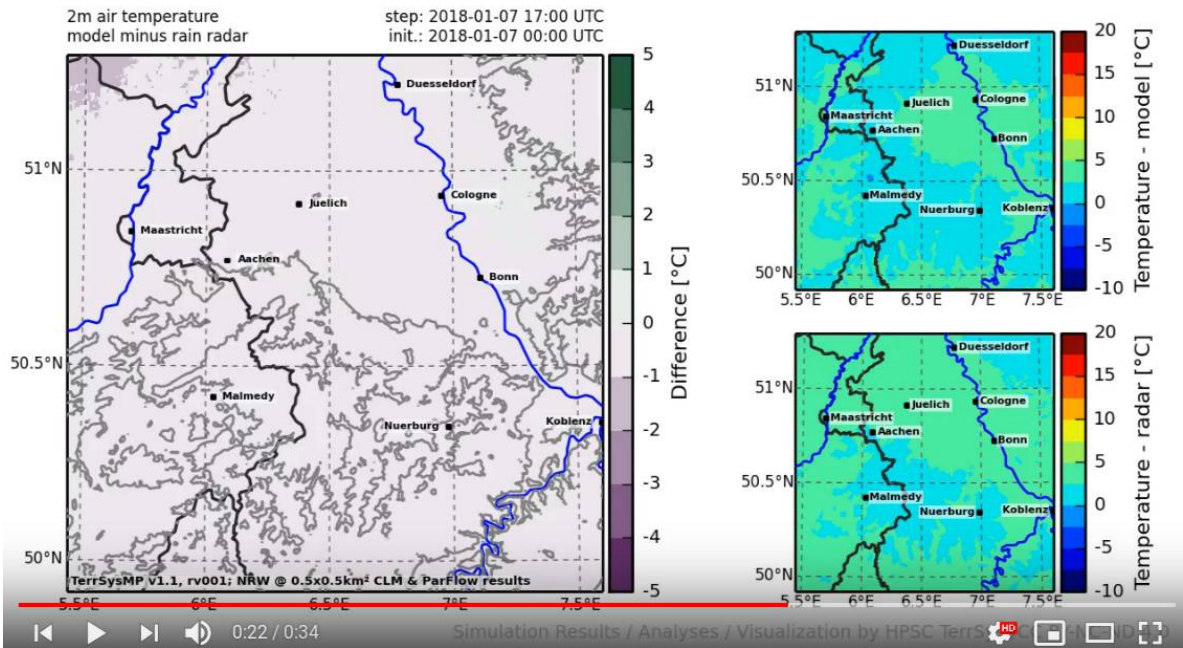
495 **Figure 11.** Difference plot for 2m air temperature [oC] between uncorrected and precipitation
496 radar corrected simulations. The panels on the right show the temperatures from the uncorrected
497 (top) and precipitation radar corrected simulations (bottom).
498
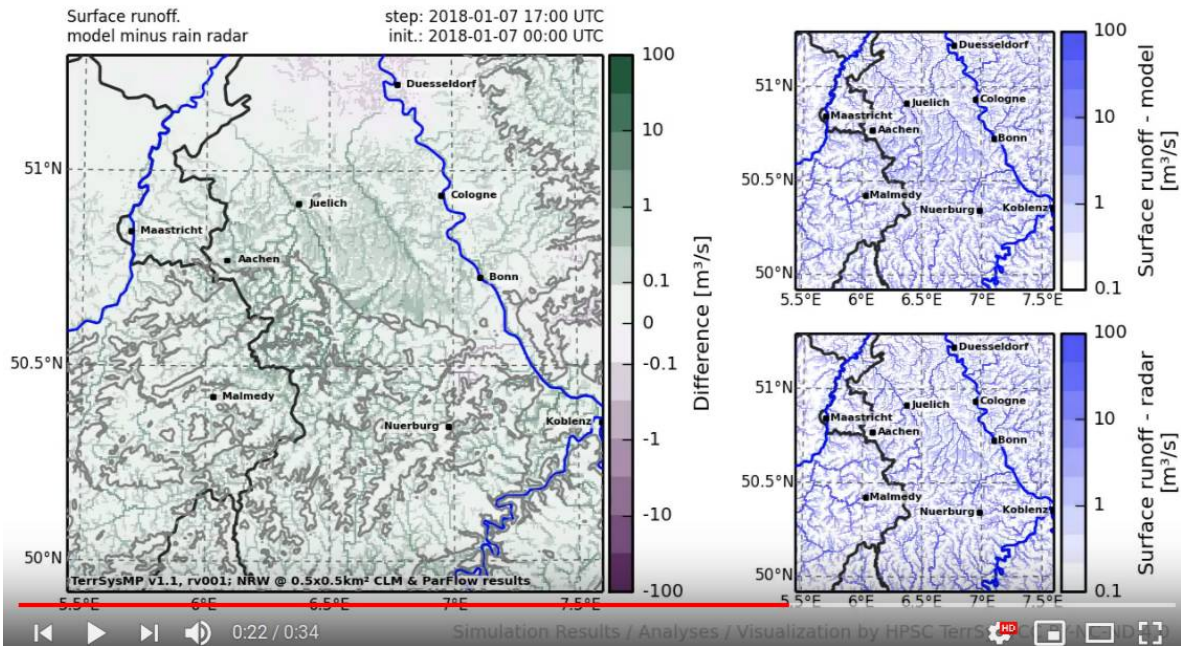
499
500
501 **Figure 12.** Difference plot for surface runoff [m3s-1] between uncorrected and precipitation
502 radar corrected simulations. The panels on the right show the runoff from the uncorrected (top) and
503 precipitation radar corrected simulations (bottom).

504 **5. Summary and conclusions**

505 We presented a real-time terrestrial monitoring system (TMS) that closes the water and energy
506 cycles from the groundwater into the atmosphere. The system provides forecasts of all states and
507 fluxes of the water and energy cycle and a physically consistent digital image of the terrestrial
508 system. The TMS has been implemented over a European continental domain (EU) and a regional
509 domain covering parts of North Rhine Westphalia and bordering countries (NRW). In case of NRW,
510 a correction of the hydrologic states is achieved by ingesting precipitation radar information into the
511 monitoring system in an offline correction run, in order to improve the initialization of the land
512 component of the ensuing monitoring run. The terrestrial monitoring system is experimental and
513 still requires comprehensive validation, which is subject of ongoing research. The system gained
514 some attention in the community and beyond. For example, the videos were watched more than
515 26,000 times since the commencement in January 2016. There is great potential in extending the
516 monitoring to e.g. the seasonal time scale, adding data assimilation for improved model
517 initialization, and the development of monitoring products for industry and public sectors. The
518 complete runtime system and output is provided freely via sftp (for access contact corresponding
519 author).

520 **Author Contributions:** Conceptualization, S.K., C.S. and K.G; methodology, S.K., C.S. and K.G; software, V.K.
521 and F.G.; formal analysis, S.K., F.G., K.G.; investigation, S.K., F.G., K.G.; data curation, F.G.; writing—original
522 draft preparation, F.G., S.K.; writing—review and editing, S.K., F.G., S.B., K.G., H.-J. H.-F., J.K., W.K., V.K., F.P.,
523 S.P., S.T, P.S., C.S., M.S.; visualization, X.X.; supervision, S.K.; project administration, S.K.; funding acquisition,
524 S.K., C.S.

525 **Funding:** This research work was supported by the SFB/TR32 Patterns in Soil-Vegetation-Atmosphere Systems:
526 Monitoring, Modeling and Data Assimilation project funded by the Deutsche Forschungsgemeinschaft (DFG)
527 and TERENO.

528 **Acknowledgments:** The authors gratefully acknowledge the computing time granted through the Board of
529 Directors on the supercomputer JURECA and JQUEEN at Forschungszentrum Jülich. We gratefully
530 acknowledge the provision of the atmospheric boundary data by the European Centre for Medium-range
531 Weather Forecasting and the German Weather Service.

532 **Conflicts of Interest:** The authors declare no conflict of interest.

References

534 1. Swinbank, R., Kyouda, M., Buchanan, P., Froude, L., Hamill, T.M., Hewson, T.D., Keller, J.H., Matsueda,
535   M., Methven, J., Pappenberger, F., Scheuerer, M., Titley, H.A., Wilson, L., Yamaguchi, M. The TIGGE
536   Project and Its Achievements. *Bull. Amer. Meteor. Soc.* **2015**, 97, 49–67.
537   https://doi.org/10.1175/BAMS-D-13-00191.1

538 2. Damrath, U., Doms, G., Frühwald, D., Heise, E., Richter, B., Steppeler, J. Operational quantitative
539   precipitation forecasting at the German Weather Service. *J. Hydrol.* **2000**, 239, 260–285.
540   https://doi.org/10.1016/S0022-1694(00)00353-X

541 3. Palmer, T. The ECMWF Ensemble Prediction System: Looking Back (more than) 25 Years and Projecting
542   Forward 25 Years. **2018**. arXiv:1803.06940 [physics]

543 4. Lynch, P. The origins of computer weather prediction and climate modeling. *J. Comp. Phys.*, **2008**,
544   Predicting weather, climate and extreme events 227, 3431–3444. https://doi.org/10.1016/j.jcp.2007.02.034

545 5. Bauer, P., Thorpe, A., Brunet, G. The quiet revolution of numerical weather prediction. *Nature* **2015**, 525,
546   47–55. https://doi.org/10.1038/nature14956

547 6. Saha, S., Moorthi, S., Wu, X., Wang, J., Nadiga, S., Tripp, P., Behringer, D., Hou, Y.-T., Chuang, H., Iredell,
548   M., Ek, M., Meng, J., Yang, R., Mendez, M.P., van den Dool, H., Zhang, Q., Wang, W., Chen, M., Becker, E.
549   The NCEP Climate Forecast System Version 2. *J. Climate* **2013**, 27, 2185–2208.
550   https://doi.org/10.1175/JCLI-D-12-00823.1

551 7. Roebber, P.J., Schultz, D.M., Colle, B.A., Stensrud, D.J. Toward Improved Prediction: High-Resolution and
552   Ensemble Modeling Systems in Operations. *Wea. Forecasting* **2004**, 19, 936–949.
553   https://doi.org/10.1175/1520-0434(2004)019<0936:TIPHAE>2.0.CO;2

554 8. Roo, A.P.J. de, Gouweleeuw, B., Thielen, J., Bartholmes, J., Bongioannini-Cerlini, P., Todini, E., Bates, P.D.,
555   Horritt, M., Hunter, N., Beven, K., Pappenberger, F., Heise, E., Rivin, G., Hils, M., Hollingsworth, A.,
556   Holst, B., Kwadijk, J., Reggiani, P., Dijk, M.V., Sattler, K., Sprokkereef, E. Development of a European
557   flood forecasting system. *Intern. J. River Basin Management* **2003**, 1, 49–59.
558   https://doi.org/10.1080/15715124.2003.9635192

559 9. Thielen, J., Bartholmes, J., Ramos, M.-H., de Roo, A. The European Flood Alert System – Part 1: Concept
560   and development. *Hydrol. Earth Syst. Sci.* **2009**, 13, 125–140. https://doi.org/10.5194/hess-13-125-2009

561 10. Refsgaard, J.C. Validation and Intercomparison of Different Updating Procedures for Real-Time
562   Forecasting. *Hydrol. Res.* **1997**, 28, 65–84. https://doi.org/10.2166/nh.1997.0005

563 11. Emerton, R., Zsoter, E., Arnal, L., Cloke, H.L., Muraro, D., Prudhomme, C., Stephens, E.M., Salamon, P.,
564   Pappenberger, F. Developing a global operational seasonal hydro-meteorological forecasting system:
565   GloFAS-Seasonal v1.0. *Geosci. Model Dev.* **2018**, 11, 3327–3346. https://doi.org/10.5194/gmd-11-3327-2018

566 12. Shukla, S., McNally, A., Husak, G., Funk, C. A seasonal agricultural drought forecast system for
567   food-insecure regions of East Africa. *Hydrol. Earth Syst. Sci.* **2014**, 18, 3907–3921.
568   https://doi.org/10.5194/hess-18-3907-2014

569 13. De Lange, W.J., Prinsen, G.F., Hoogewoud, J.C., Veldhuizen, A.A., Verkaik, J., Oude Essink, G.H.P., van
570   Walsum, P.E.V., Delsman, J.R., Hunink, J.C., Massop, H.T.L., Kroon, T. An operational, multi-scale,
571   multi-model system for consensus-based, integrated water management and policy analysis: The
572   Netherlands Hydrological Instrument. *Env. Mod. & Soft.* **2014**, 59, 98–108.
573   https://doi.org/10.1016/j.envsoft.2014.05.009

574 14. Shrestha, P., Sulis, M., Masbou, M., Kollet, S., Simmer, C. A Scale-Consistent Terrestrial Systems Modeling
575   Platform Based on COSMO, CLM, and ParFlow. *Mon. Wea. Rev.* **2014**, 142, 3466–3483.
576   https://doi.org/10.1175/MWR-D-14-00029.1

577 15. Gasper, F., Goergen, K., Shrestha, P., Sulis, M., Rihani, J., Geimer, M., Kollet, S. Implementation and
578   scaling of the fully coupled Terrestrial Systems Modeling Platform (TerrSysMP v1.0) in a massively
579   parallel supercomputing environment – a case study on JUQUEEN (IBM Blue Gene/Q). *Geosci. Mod. Dev.*
580   **2014** 7, 2531–2543. https://doi.org/10.5194/gmd-7-2531-2014

16. Simmer, C., I. Thiele-Eich, M. Masbou, W. Amelung, S. Crewell, B. Diekkrueger, F. Ewert, H.-J. Hendricks Franssen, A. J. Huisman, A. Kemna, N. Klitzsch; S. Kollet, M. Langensiepen, U. Loehnert, M. Rahman, U. Rascher, K. Schneider, J. Schween, Y. Shao, P. Shrestha, M. Stiebler, M. Sulis, J. Vanderborght, H. Vereecken, J. van der Kruk, T. Zerenner, and G. Waldhoff. Monitoring and Modeling the Terrestrial System from Pores to Catchments - the Transregional Collaborative Research Center on Patterns in the Soil-Vegetation-Atmosphere System. *Bull. Am. Meteorol. Soc.* **2014**, 96, 1765–1787. doi: http://dx.doi.org/10.1175/BAMS-D-13-00134.1

17. Rahman, M., Sulis, M., Kollet, S.J. The concept of dual-boundary forcing in land surface-subsurface interactions of the terrestrial hydrologic and energy cycles. *Wat. Resour. Res.* **2014**, 50, 8531–8548. https://doi.org/10.1002/2014WR015738

18. Rahman, M., M. Sulis, and S.J. Kollet. The subsurface-land surface-atmosphere connection under convective conditions, *Adv. in Water Resour.* **2015**, 83, 240-249.

19. Keune, J., F. Gasper, K. Goergen, A. Hense, P. Shrestha, M. Sulis, and S. Kollet. Studying the influence of groundwater representations on land surface-atmosphere feedbacks during the European heat wave in 2003, J. *Geophys. Res. Atmos.* **2016**, 121, 13, 301–13,325, doi:10.1002/2016JD025426. doi:10.1002/2016JD025426.

20. Sulis, M., Williams, J.L., Shrestha, P., Diederich, M., Simmer, C., Kollet, S.J., Maxwell, R.M. Coupling Groundwater, Vegetation, and Atmospheric Processes: A Comparison of Two Integrated Models. *J. Hydrometeor.* **2017**, 18, 1489–1511. https://doi.org/10.1175/JHM-D-16-0159.1

21. Sulis, M., J. Keune, P. Shrestha, C. Simmer, and S. J. Kollet. Quantifying the Impact of Subsurface-Land Surface Physical Processes on the Predictive Skill of Subseasonal Mesoscale Atmospheric Simulations. *J. Geophys. Res. Atmos.* **2018**, 123(17), 9131-9151, DOI: 10.1029/2017JD028187.

22. Keune, J., Sulis, M., Kollet, S., Siebert, S., Wada, Y. Human Water Use Impacts on the Strength of the Continental Sink for Atmospheric Water. *Geophys. Res. Let.* **2018**, 45, 4068–4076. https://doi.org/10.1029/2018GL077621

23. Keune, J., Sulis, M., Kollet, S, Potential added value of incorporating human water use in the simulation of evapotranspiration and precipitation in a continental-scale bedrock-to-atmosphere modeling system. *J. Adv. Modeling Earth Sys.* (under review)

24. Baldauf, M., Seifert, A., Förstner, J., Majewski, D., Raschendorfer, M., Reinhardt, T. Operational Convective-Scale Numerical Weather Prediction with the COSMO Model: Description and Sensitivities. *Mon. Wea. Rev.* **2011**, 139, 3887–3905. https://doi.org/10.1175/MWR-D-10-05013.1

25. Oleson, K.W., Niu, G.-Y., Yang, Z.-L., Lawrence, D.M., Thornton, P.E., Lawrence, P.J., Stöckli, R., Dickinson, R.E., Bonan, G.B., Levis, S., Dai, A., Qian, T. Improvements to the Community Land Model and their impact on the hydrological cycle. *J. Geophys. Res: Biogeosci* **2008**, 113. https://doi.org/10.1029/2007JG000563

26. Jones, J.E., Woodward, C.S. Newton–Krylov-multigrid solvers for large-scale, highly heterogeneous, variably saturated flow problems. *Adv. Water Resour.* **2001**, 24, 763–774. https://doi.org/10.1016/S0309-1708(00)00075-0

27. Kollet, S.J., Maxwell, R.M., 2006. Integrated surface–groundwater flow modeling: A free-surface overland flow boundary condition in a parallel groundwater flow model. Advances in Water Resources 29, 945–958. https://doi.org/10.1016/j.advwatres.2005.08.006

28. Maxwell, R.M. A terrain-following grid transform and preconditioner for parallel, large-scale, integrated hydrologic modeling. *Adv. Water Resour.* **2013**, 53, 109–117. https://doi.org/10.1016/j.advwatres.2012.10.001

29. Valcke, S. The OASIS3 coupler: a European climate modelling community software. *Geosci. Model Dev.* **2013**, 6, 373–388. https://doi.org/10.5194/gmd-6-373-2013

30. Rodwell, M.J., Magnusson, L., Bauer, P., Bechtold, P., Bonavita, M., Cardinali, C., Diamantakis, M., Earnshaw, P., Garcia-Mendez, A., Isaksen, L., Källén, E., Klocke, D., Lopez, P., McNally, T., Persson, A., Prates, F., Wedi, N. Characteristics of Occasional Poor Medium-Range Weather Forecasts for Europe. *Bull. Amer. Meteor. Soc.* **2013**, 94, 1393–1405. https://doi.org/10.1175/BAMS-D-12-00099.1

31. Kurtz, W., He, G., Kollet, S. J., Maxwell, R. M., Vereecken, H., and Hendricks Franssen, H.-J. TerrSysMP–PDAF (version 1.0): a modular high-performance data assimilation framework for an integrated land surface–subsurface model. *Geosci. Model Dev.* **2016**, 9, 1341-1360, doi:10.5194/gmd-9-1341-2016.

633 32. Zhang, H., Kurtz, W, Kollet, S., Vereecken, H. Hendricks Franssen, H.J. Comparison of different
634   assimilation methodologies of groundwater levels to improve predictions of root zone soil moisture with
635   an integrated terrestrial systems model. *Adv. Water Resour.* **2018**, 111, 224-238.

636 33. Diederich, M., A. Ryzhkov, C. Simmer, P. Zhang, and S. Troemel. Use of specific attenuation for rainfall
637   measurement at X-band radar wavelengths - Part 1: Radar calibration and partial beam blockage
638   estimation. *J. Hydrometeor.* **2015**, 16(2), 487-502, https://doi.org/10.1175/JHM-D-14-0066.1

639 34. Diederich, M., Ryzhkov, A., Simmer, C., Zhang, P., Trömel, S. Use of Specific Attenuation for Rainfall
640   Measurement at X-Band Radar Wavelengths. Part II: Rainfall Estimates and Comparison with Rain
641   Gauges. *J. Hydrometeor.* **2015**, 16(2), 503–516. https://doi.org/10.1175/JHM-D-14-0067.1

642 35. Schättler, U. and U. Blahak, A Description of the Nonhydrostatic Regional COSMO-Model Part V:
643   Preprocessing: Initial and Boundary Data for the COSMO-Model. 2018. Available online:
644   http://www.cosmo-model.org/content/model/documentation/core/int2lm_2.03.pdf   (accessed   on
645   23.10.2018).